Toughness of Glassy−Semicrystalline Multiblock Copolymers

Alhad Phatak, Lisa S. Lim, Cletis K. Reaves, and Frank S. Bates*

Department of Chemical Engineering and Materials Science, University of Minnesota, Minneapolis, Minnesota 55455

Received May 19, 2006; Revised Manuscript Received July 4, 2006

ABSTRACT: We report a study on the mechanical properties of lamellae-forming glassy−semicrystalline block copolymers composed of poly(cyclohexylethylene) (C) and polyethylene (E). Tensile properties of polydomain CEC, ECEC, CECEC, and ECECE block copolymers, and blends of these materials, reveal a critical dependence on the connectivity of the semicrystalline E blocks. A molecular parameter directly related to the fraction of bridging E blocks is identified, which captures the fracture behavior of C/E block copolymers over a range of chain architectures. Tensile testing and small-angle X-ray scattering (SAXS) experiments on aligned block copolymers reveal the role of bridging in the glassy C block and further elucidate the mechanisms that govern the deformation of microphase-separated lamellar domains and macroscopic fracture in glassy−semicrystalline block copolymers.

Introduction

Polystyrene (S)-based block copolymers have been widely used as thermoplastic elastomers and plastics, combining the stiffness of polystyrene with the ductility of a rubbery component (polyisoprene (I), polybutadiene (B)).[1−3] Thermoplastic elastomers (SBS and SIS triblock copolymers) contain polybutadiene or polyisoprene as the continuous domain, while dispersed polystyrene domains (typically cylinders or spheres) act as physical cross-links. Partially hydrogenated SBS and SIS block copolymers also have been successful commercially. Plastics such as K-Resins contain polystyrene-rich $(SB)_n$ multiblock copolymers and function as clear, high modulus, and high impact strength materials.[4]

Hydrogenation of unsaturated block copolymers provides a potentially inexpensive way to enhance the chemical, thermal, and UV stability of these materials. In addition, hydrogenation of polystyrene ($T_g \approx 100$ °C) to poly(cyclohexylethylene) (PCHE or C, $T_g \approx 145$ °C) raises the upper use temperature significantly.[5] Virtually complete (>99%) hydrogenation of polystyrene requires relatively small amounts of a platinum-based catalyst.[6] Incorporation of PCHE (which is a brittle polymer due to a high entanglement molecular weight, $M_{e,C} \approx 40$ kg/mol[7]) into block copolymers with polyethylene (PE or E; hydrogenated polybutadiene) has led to the development of C/E glassy−semicrystalline block copolymers, with potential applications that transcend traditional thermoplastic elastomers and plastics. These materials display a variety of desirable properties, notably excellent optical clarity.[8] C and E blocks are relatively incompatible (evidenced by a Flory−Huggins interaction parameter, $\chi = 0.052$ at 150 °C[9]) and readily form microphase-separated structures, providing good model systems for studying the interplay between glassy and semicrystalline components.

The mechanical properties of lamellae[10−12] and cylinder[12−15] forming CEC and CECEC block copolymers have been actively studied in the past few years. Much of this work has focused on the consequences of including the center C block in the pentablock material. The presence of bridging conformations in the pentablock center C block has been shown to result in mechanical properties that are superior to the corresponding CEC triblock material. In macroscopically aligned lamellar specimens, Mori et al. found that adding just 10% CECEC to neat CEC dramatically alters the mechanical response from brittle failure to ductile deformation when stress is applied normal to the plane of the lamellae.[10] They also demonstrated agreement with the estimated amount of CECEC necessary to effect this change, based on the force required to break individual C chains.[16] However, the role of chain conformations in the E block has not been evaluated. In the CEC and CECEC systems, all E blocks are anchored at C/E interfaces. Brittleness of CE and ECE block copolymers has been attributed to the absence of such flexible chains "connecting" brittle C domains.[17] SB, BSB, SI, and ISI block copolymers also have been reported to have inferior tensile properties compared to SBS and SIS triblocks, presumably for the same reasons.[18,19] While these studies underscore the importance of rubbery chains linking rigid glassy domains, an explanation that systematically addresses the integrated roles of chain architecture (number of blocks, block sequence), morphology, chain conformations, and microstructure orientation in determining fracture in this class of compounds remains elusive. One-dimensional lamellae provide an ideal morphology for studying mechanical properties: (i) well-aligned specimens can be generated through dynamic shearing,[20] (ii) structure−property correlation is simplified due to the one-dimensional structural geometry, and (iii) lamellae better expose mechanical contributions from each component vs other classical morphologies (cylinders, spheres) which tend to be dominated by the majority (matrix) phase.

In this paper, we provide molecular level insight into the mechanical response of lamellae-forming C/E block copolymers. We employ CEC, ECEC, and ECECE architectures as well as blends of these compounds to control the extent of bridging chains in the semicrystalline domains. Tensile properties of isotropic samples are first described, and the results are rationalized on the basis of the amount of bridging chains in the semicrystalline block. Experiments on macroscopically aligned lamellae are used to probe mechanical properties in different directions relative to the bulk lamellar orientation. Properties of oriented samples reveal the contribution of each orientation to the overall isotropic response.

* Corresponding author. E-mail: bates@cems.umn.edu.

10.1021/ma0611319 CCC: $33.50
Published on Web 08/08/2006

Table 1. Molecular and Structural Characteristics of C/E Block Copolymers

polymer[a]	M_n, kg/mol[b]	PDI[c]	volume fraction PCHE (f_C)[d]	$N_{2,E}/N_{1,E}$[e]	T_{ODT}, °C[f]	lamellae periodicity (d*), nm[g]	% crystallinity in PE block (x_c)[h]
CEC-1*	34.5	1.12	0.52		262	17.9	16
CEC-2*	35.5	1.15	0.57		243	17.6	16
CECEC*	54.4	1.09	0.52	1.0	231	16.7	18
ECEC-1	34.3	1.15	0.45	1.0	253	19.8	27
ECECE-5	48.9	1.17	0.61	1.1	205	18.3	24
ECECE-10	41.1	1.25	0.42	2.6	255	18.4	21

[a] Polymers indicated by asterisks were provided by Dow Chemical Company. [b] Based on molecular weight of the first block (determined by SEC) and composition of unsaturated precursor (determined by ^{1}H NMR). [c] Determined by high-temperature SEC with TCB as mobile phase. [d] Determined by ^{1}H NMR. [e] Based on amounts of butadiene monomer added in the first and second steps of butadiene addition in the sequential anionic polymerization procedure. [f] Determined by dynamic mechanical analysis. [g] Determined by SAXS. [h] Determined by DSC.

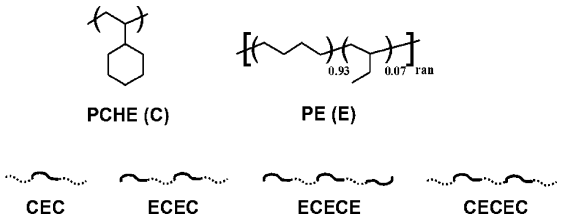

Figure 1. Molecular structures of poly(cyclohexylethylene) (C) and polyethylene (E) and the chain architectures of the block copolymers used in this study. C and E are denoted by dotted and solid lines, respectively.

Experimental Section

Synthesis of Block Copolymers. Unsaturated poly(styrene-*b*-butadiene) $(S-B)_n$ multiblock copolymers were synthesized by sequential anionic polymerization reactions initiated by *sec*-butyllithium in cyclohexane at 40 °C using previously documented techniques.[21] Rigorously purified styrene and butadiene monomers were added sequentially to an alkyllithium solution and allowed to react for 6−8 h per block to obtain SBS, BSBS, SBSBS, and BSBSB block copolymers. These conditions led to ~93% 1,4 (~7% 1,2) polybutadiene addition by weight, as determined by ^{1}H nuclear magnetic resonance (NMR) measurements. Saturated CEC, ECEC, CECEC, and ECECE block copolymers were obtained by hydrogenating the corresponding unsaturated precursors in cyclohexane at 170 °C and 500 psi over a silica supported Pt/Re catalyst for 8 h.[6] Illustrations of the resulting molecular structures are provided in Figure 1, and molecular characteristics of the block copolymers used in this study are listed in Table 1. ECECE-10 has a center-to-end E block degree of polymerization ratio ($N_{2,E}/N_{1,E}$) greater than 1, while the other polymers have equal-sized E blocks ($N_{2,E}/N_{1,E} \approx 1$). Molecular weights of the polymers were established by a combination of size exclusion chromatography (SEC) performed on aliquots of the first block taken from the reaction mixture and overall compositions obtained from ^{1}H NMR.

Preparation of Block Copolymer Blends. CEC/ECEC and CEC/ECECE blends were prepared by codissolving the constituent polymers in toluene at 90 °C. The blends were recovered by precipitation in methanol followed by drying under dynamic vacuum.

Molecular Characterization. SEC measurements on the unsaturated precursors were performed at room temperature with a Waters 717 system using tetrahydrofuran (THF) as the mobile phase, while the saturated polymers were analyzed at 140 °C in trichlorobenzene (TCB) on a PL-GPC 220 system. Both these SEC systems are equipped with refractive index detectors. ^{1}H NMR measurements were conducted at room temperature in deuterated chloroform and at 70 °C in deuterated toluene for the unsaturated and saturated polymers, respectively, using a Varian Inova 300 spectrometer.

Differential Scanning Calorimetry (DSC). DSC measurements were conducted on a TA Instruments Q1000 system using heating and cooling rates of 10 °C/min to obtain melting points (T_m) and degrees of crystallinity (x_c) in the semicrystalline E domains.

Rheology. Linear dynamic mechanical spectroscopy (DMS) measurements were performed with a Rheometric Scientific ARES rheometer, using 25 mm parallel plates. Isochronal ($\omega = 1$ rad/s) measurements were conducted while heating and cooling at 2 °C/min, while isothermal dynamic frequency sweep experiments were run at frequencies ranging from $\omega = 0.1$ to 100 rad/s at various temperatures. All DMS measurements were performed under a nitrogen atmosphere, at a strain amplitude of 1%, which was found to be within the linear viscoelastic regime for each polymer.

Small-Angle X-ray Scattering (SAXS). SAXS was used to characterize the morphology and microstructure orientation in block copolymer samples at room temperature. These measurements were performed by exposing samples to 1.54 Å wavelength Cu Kα radiation for 10 min, and two-dimensional scattering patterns were collected with a Siemens area detector located 230 cm from the sample.

Sample Preparation for Tensile Testing. Saturated block copolymers and blends were compression molded into ~1 mm thick rectangular sheets at 200 °C.

Isotropic (Polydomain) Samples. To obtain isotropic samples, the pressed sheets were annealed in the disordered state (T_{ODT} + 10 °C) for 15 min before cooling to room temperature. Tensile bars with dimensions ~8 mm × 3 mm × 1 mm were sectioned using scissors, and SAXS measurements were used to establish the distribution of lamellae prior to tensile testing.

Aligned Samples. Pressed samples were processed using a reciprocating shear device[22] by following a "shear from disorder" protocol described elsewhere[23] to induce macroscopic perpendicular alignment of lamellae. Orientation was determined by SAXS before sectioning ~8 mm × 3 mm × 1 mm bars for tensile testing.

Tensile Testing. Uniaxial tensile testing experiments were performed at room temperature using a Rheometric Scientific Minimat instrument at a crosshead speed of 8 mm/min ("length-independent" rate of 1 min^{-1}). At least five tensile measurements were performed for each sample. ECEC-1 and ECECE-5 samples were too brittle to be gripped using this instrument, and tensile tests for these materials were performed with a Perkin-Elmer dynamic mechanical analyzer (DMA-7e) stress-controlled rheometer operated at 300 mN/min. Rectangular samples having dimensions 4 mm × 2 mm × 1 mm were used in the DMA-7e.

Results and Analysis

Molecular and Structural Characterization. Table 1 lists the molecular and structural characteristics of the saturated block copolymers used in this study. Block copolymer compositions were established from ^{1}H NMR spectra obtained from the S/B precursors.[24,25] The absence of resonances corresponding to styrene and butadiene in the ^{1}H NMR spectra obtained from the C/E block copolymers indicated nearly complete hydrogenation.

As can be seen from Table 1, T_{ODT} values (identified through DMS by a precipitous drop in elastic modulus during isochronal temperature ramp measurements[26]) in all cases are above the C block glass transition and E block crystallization temperatures ($T_{ODT} > T_{g,C}, T_{m,E}$). 2-D SAXS data obtained at room temper-

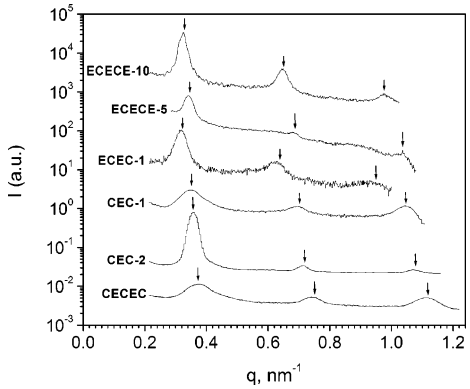

Figure 2. 1-D SAXS profiles obtained at room temperature from C/E block copolymers. The vertical arrows denote peak locations expected for a lamellar microstructure.

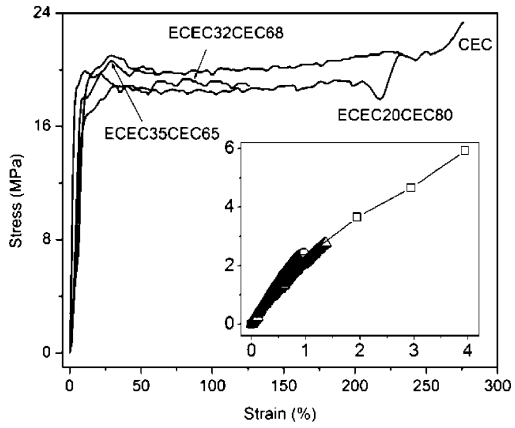

Figure 3. Representative stress−strain curves obtained from CEC-1, ECEC20CEC80, ECEC32CEC68, and ECEC35CEC65 materials. The inset shows representative tensile data obtained from ECEC80CEC20 (□), ECEC-1 (△), and ECECE-5 (○).

ature were integrated azimuthally to yield scattering intensity (I) profiles as a function of scattering wavevector $q = (4\pi/\lambda)\sin(\theta/2)$, where θ is the scattering angle and λ (= 1.54 Å) is the X-ray wavelength. Figure 2 shows I vs q data for all the polymers employed in this study. All curves show a primary scattering peak (q^*) and higher order reflections at $2q^*$ and $3q^*$, which indicate that the polymers microphase separate into a lamellar morphology.[27] The lamellae periodicities (d^*) calculated from the locations of the primary peak, $d^* = 2\pi/q^*$, lie between 17 and 20 nm for all these block copolymers. DSC experiments were used to measure the heats of melting (ΔH_m) of the PE crystals. The degrees of crystallinity (x_c) were calculated on the basis of the theoretical heat of fusion for a 100% crystalline polyethylene of $\Delta H_{f,th} = 277$ J/g[28] with $x_c = (100\Delta H_m)/(\Delta H_{f,th} w_E)$, where w_E is the weight fraction of PE in the block copolymer. The results show a discernibly higher degree of PE crystallinity in the ECEC and ECECE materials, which have "loose" E end blocks. The tethering of E blocks at both ends in the CEC and CECEC architectures likely restricts the extent of PE crystallization within the microphase-separated lamellar domains, leading to lower x_c values. This is consistent with the results of Weimann et al., who reported higher degrees of crystallinity for CE diblock vs CEC triblock copolymers.[29]

Tensile Properties of Isotropic Block Copolymers. Uniaxial tensile testing was employed to measure the room temperature deformation behavior of isotropic C/E block copolymers. Engineering stress (σ) and strain (ϵ) values were obtained from force and displacement measurements and initial sample dimensions. Figure 3 shows representative stress−strain curves obtained from CEC-1, ECEC-1, and ECECE-5 specimens. All three polymers show little difference in the elastic moduli (low strain region), which are likely dependent solely on the block copolymer composition. Both ECEC-1 and ECECE-5 display elastic deformation followed by brittle failure at very low strains ($\epsilon_f \approx 1\%$). On the other hand, CEC-1 shows an initial elastic region followed by necking and strain hardening before ultimately breaking at a strain of nearly 300%. This clearly demonstrates the consequences of altering the arrangement of chains across the lamellar microstructure. In the CEC block copolymer, all the E blocks must necessarily adopt looped or bridged conformations (i.e., they are "tied down"), whereas 50% of the PE chains in ECEC and 67% of the PE chains in ECECE are free at one end. To further understand the effect of tying down the soft block, we blended CEC-1 with ECEC-1 and ECECE-5 to produce a series of samples having varying amounts of "tied down" PE chains. Stress−strain experiments for both CEC/ECEC and CEC/ECECE blends revealed an abrupt transition from brittle to ductile behavior with the addition of CEC block copolymer. For the sake of clarity, we have only included CEC/ECEC tensile data in Figure 3 and omitted the stress−strain curves obtained from the CEC/ECECE samples. From the amounts of each species used to prepare blend samples, and the respective PE block molecular weights, the weight fraction of tied down PE chains, or ψ_E, is given by

$$\psi_E = \begin{cases} \dfrac{n_{CEC}M_{E,CEC} + n_{ECEC}M_{E,ECEC}}{n_{CEC}M_{E,CEC} + 2n_{ECEC}M_{E,ECEC}} & \text{for CEC/ECEC blends} \\ \dfrac{n_{CEC}M_{E,CEC} + n_{ECECE}M_{E,ECECE}}{n_{CEC}M_{E,CEC} + 3n_{ECECE}M_{E,ECECE}} & \text{for CEC/ECECE blends} \end{cases}$$

Here, $M_{E,X}$ denotes the molecular weight of a PE block in block copolymer X and n_X denotes the number fraction of chains of block copolymer X in a blend. Table 2 lists the compositions and ψ_E values for the blends employed. We have described the variation of failure strain using the single parameter ψ_E, which can be defined for any C/E block copolymer or blend. Figure 4 shows the variation of ϵ_f with ψ_E for all the block copolymers and blends studied in this work. This plot also includes results from the literature for CE, ECE, CEC-2, and CECEC block copolymers.[17,30] The open triangle in this plot represents the ECECE-10 material, which is addressed in the next section.

Table 2. Compositions of ECEC−CEC and ECECE−CEC Blends

blend name	wt % CEC	wt % ECEC-1	wt % ECECE-5	ψ_E
ECECE-5			100	0.33
ECEC-1		100		0.50
CEC	100			1.00
ECEC80CEC20	20	80		0.59
ECEC40CEC60	60	40		0.79
ECEC35CEC65	65	35		0.81
ECEC32CEC68	68	32		0.83
ECEC20CEC80	80	20		0.89
ECECE60CEC40	40		60	0.66
ECECE50CEC50	50		50	0.72
ECECE40CEC60	60		40	0.78
ECECE35CEC65	65		35	0.81
ECECE30CEC70	70		30	0.84

Tensile Properties of Oriented Block Copolymers. Oriented, "single crystal" samples were prepared by subjecting the block copolymers to reciprocating shear flow applied via parallel plates. Specimens were first held in the disordered state (T_{ODT}

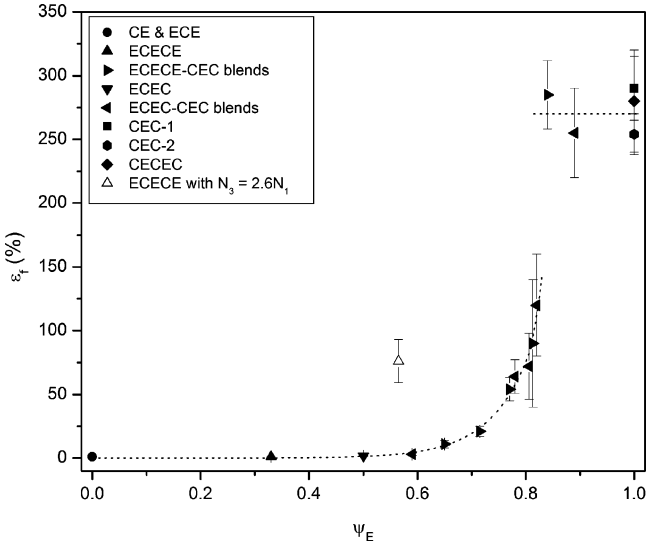

Figure 4. Failure strain (ϵ_f) as a function of ψ_E for a number of C/E block copolymer architectures. The open triangle denotes ECECE-10. The dotted lines are provided to guide the eye.

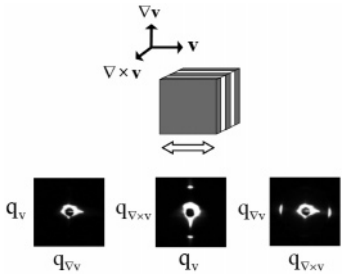

Figure 5. Schematic of a lamellae-forming block copolymer oriented in the perpendicular alignment. The horizontal arrow denotes the shear direction. 2-D SAXS patterns with the X-ray beam directed along vorticity, velocity gradient, and flow directions are shown at the bottom.

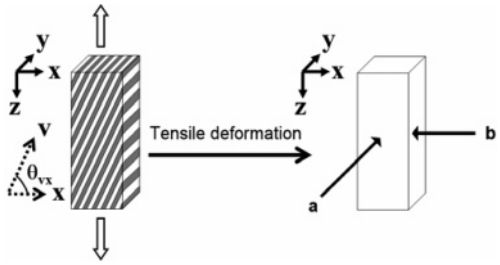

Figure 6. Schematic showing the lamellar orientation relative to the strain direction before tensile deformation (defined by the angle θ_{vx}).

+ 7 °C) for 10 min, followed by simultaneous application of shear and cooling at ~5 °C/min to the ordered state (T_{ODT} − 30 °C). Shearing was stopped after 1 h, and the samples were cooled to room temperature at ~1.5 °C/min. Figure 5 depicts the perpendicular lamellar alignment with respect to the velocity (v), gradient (∇v), and vorticity($\nabla \times v$) directions associated with the shear flow field.[20] Representative 2-D SAXS patterns obtained with the X-ray beam directed at each of the three orthogonal faces of sheared specimens confirm perpendicular alignment of lamellae. Note that the coordinate system defined by mutually orthogonal directions *x*, *y*, and *z* is used to describe the tensile testing experiment (Figure 6).

Oriented ECECE-5 samples were found to be equally brittle ($\epsilon_f \approx 1\%$) when strained along the lamellae normal and parallel

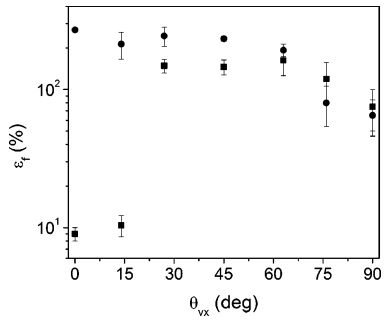

Figure 7. Failure strain (ϵ_f) as a function of lamellar orientation (defined by θ_{vx}) for (■) CEC and (●) CECEC block copolymers.

to the plane of the lamellae; i.e., there is very little orientation dependence to the failure strain. We use θ_{vx} to define the strain direction relative to the lamellar orientation prior to tensile testing (see Figure 6). Figure 7 shows the variation of failure strain (ϵ_f) as a function of strain direction for the CEC and CECEC block copolymers. 2-D SAXS data taken with the beam directed along the *y* and *x* directions of the gauge sections in failed tensile samples are presented in Figures 8 and 9. For $\theta_{vx} \geq 27°$, the CEC material undergoes plastic deformation and yielding before failure, while brittle behavior is seen for smaller angles. Samples strained along $\theta_{vx} = 76°$ and 90° displayed relatively inconsistent tensile behavior evidenced by the sizable error bars in Figure 7, and failure was initiated by tearing of samples into "strands" along the strain direction. The scattering patterns obtained from the $x-z$ plane are shown in the top panel, while those obtained from the $y-z$ plane are shown in the bottom panel of Figure 8. For $\theta_{vx} = 0°$ and 14°, CEC tensile bars fail before yielding, and the lamellar structure remains unaltered as evidenced by no change in the azimuthal locations (relative to starting θ_{vx}) of the scattering peaks in the q_x-q_z plane. For $\theta_{vx} = 27°$, 45°, and 63°, the azimuthal positions of the primary scattering peaks (in the q_x-q_z plane) change, while the lamellae periodicities remain nearly unchanged ($d^* \approx 18$ nm). At these angles, no scattering is seen from the edges of failed samples. For $\theta_{vx} = 76°$ and 90°, the SAXS patterns show very weak scattering spots along the *z* direction.

The tensile properties of CECEC specimens show little orientation dependence. For $\theta_{vx} < 27°$, the CECEC pentablock exhibits dramatically higher failure strains than the CEC triblock (the $\theta_{vx} = 0°$ limit has been addressed previously[10,11]). At these angles ($\theta_{vx} = 0°$ and 14°), 2-D SAXS patterns (Figure 9) from the $y-z$ plane show four spots at the same value of q^* identified in the prestrained material. No scattering spots are seen in the q_x-q_z plane. An azimuthal "shift" of primary scattering peaks (in the q_x-q_z plane) without a change in lamellae periodicities ($d^* \approx 17$ nm) is seen for $\theta_{vx} = 27°$, 45°, and 63°. No scattering peaks are seen for $\theta_{vx} = 76°$ and 90°.

Although the two polymers are almost equally tough for $\theta_{vx} \geq 27°$, the nature of ultimate fracture is different. Pictures of failed tensile specimens (Figure 10) show that the CEC samples fail macroscopically by propagation of cracks along a single direction. Comparing the images in Figure 10 with the SAXS patterns in Figure 8, we conclude that the cracks propagate parallel to the lamellae interfaces. On the other hand, CECEC samples do not show a "preferred" failure direction, and specimens always fail close to the grips (except for $\theta_{vx} = 76°$ and 90°).

CEC-2 was used instead of CEC-1 for alignment studies because the T_{ODT} of CEC-1 is higher than the upper temperature limit for the reciprocating shear machine. However, isotropic

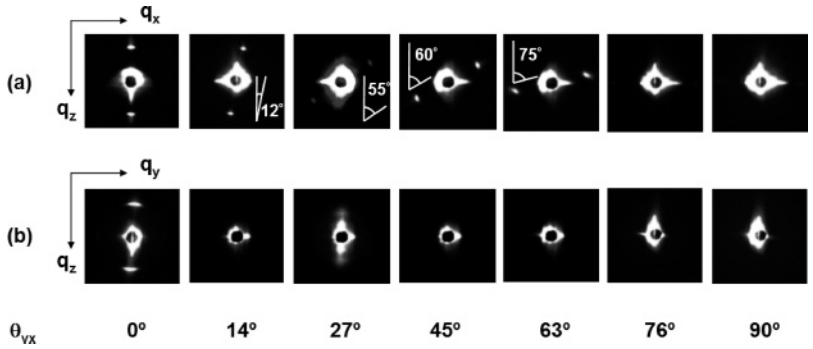

Figure 8. 2-D SAXS patterns from the (a) $x-z$ and (b) $y-z$ planes of failed CEC tensile bars strained along different directions relative to the macroscopic lamellae orientation. The "*a*" and "*b*" directions are defined in Figure 6.

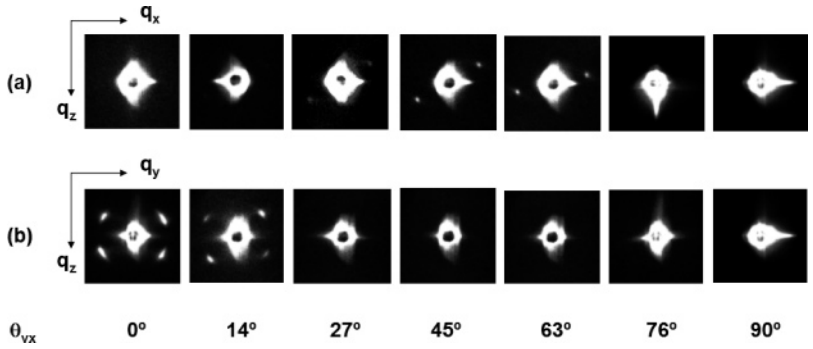

Figure 9. 2-D SAXS patterns from the (a) $x-z$ and (b) $y-z$ planes of failed CECEC tensile bars strained along different directions relative to the macroscopic lamellae orientation. The "*a*" and "*b*" directions are defined in Figure 6.

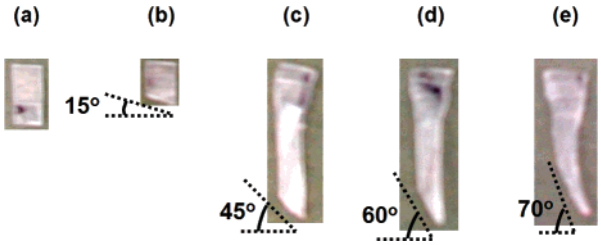

Figure 10. Representative pictures of failed CEC tensile bars strained along $\theta_{vx} =$ (a) 0°, (b) 14°, (c) 27°, (d) 45°, and (e) 63°. CEC samples ultimately fracture parallel to the lamellar interface, while CECEC samples do not display a preferred direction of failure.

samples of both polymers show nearly identical tensile properties and may be used interchangeably. Also worth mentioning is that macroscopically oriented samples obtained by extrusion of CEC-1 through a slit die[31] showed similar (as CEC-2) anisotropy in mechanical properties (brittle along the lamellae normal; ductile, parallel to the lamellar interface) but were too small to conduct a detailed study of the dependence of ϵ_f on θ_{vx}.

Discussion

Deformation of Isotropic Samples. Figure 4 summarizes the tensile behavior of a significant number of linear C/E multiblock copolymers in terms of a single parameter ψ_E. A critical ψ_E must be reached in order to obtain a C/E block copolymer (or blend) than can deform without brittle failure. It should be kept in mind that *both* PCHE and PE homopolymers, with molecular weights equal to the individual C and E blocks in our samples, are extremely brittle materials. As a result, constructing a "composite" material having a lamellar microphase-separated structure (of periodicity ~20 nm) *alone* does not lend toughness (as evidenced by brittle CE diblock). Moreover, connecting the domains by rigid PCHE chains does not reinforce the lamellar microstructure either, as evidenced by the brittle ECE triblock. To access a plastic deformation mode, the semicrystalline E domains need to be sufficiently toughened by anchoring the PE chains at C/E interfaces. In Figure 4, we can identify three different "levels" of anchoring of PE blocks. For $\psi_E < 0.6$, the PE domains are not tough enough to undergo plastic deformation, and samples fail by brittle fracture. In this limit, the lack of toughness in the PE domains controls the mechanical behavior as chain pullout from C domains may be ruled out (all C blocks are tied down in ECE and ECECE). For $0.6 < \psi_E < 0.8$, a critical fraction of PE chains adopt "tied down" conformations leading to rapid toughening ($\epsilon_f \propto \psi_E^{13.6}$) of the isotropic lamellar structure. Once there is enough connectivity across lamellae, brittle fracture is prevented by plastic deformation of the semicrystalline domains. Some of the toughness can be attributed to the isotropic structure itself (see the discussion on oriented samples below). Interestingly, in the limit of $\psi_E > 0.8$, a strain-to-failure of ca. 300% is seen regardless of chain architecture (ECEC/CEC, ECECE/CEC, CEC, and CECEC). This suggests universality in the failure mechanism in these materials. In this limit, ultimate failure likely occurs in the C blocks by chain pullout; this hypothesis is supported by experiments on aligned CEC samples discussed below. For a given ratio of block sizes, ψ_E can thus be thought of as a "predictive tool" to design new block copolymer architectures having desired toughness.

The tied down chains in the semicrystalline block can adopt two different chain conformations: loops and bridges. In lamellae-forming symmetric ABA triblock copolymers, an equilibrium bridging fraction of 0.4 is predicted by theory[32−34] and has been estimated from dielectric relaxation experiments.[35−37] Drolet and Fredrickson calculated the fraction of bridging chains

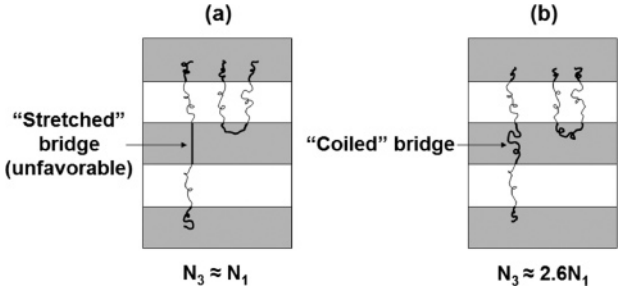

Figure 11. Proposed chain conformations in (a) ECECE-5 and (b) ECECE-10 block copolymers. The dark and light lines represent E and C blocks, respectively. Increasing $N_{2,E}/N_{1,E}$ is predicted to increase the fraction of E block bridging conformations by reducing the chain stretching penalty in the center E block.[13] For simplicity, looping conformations in the C blocks are omitted.

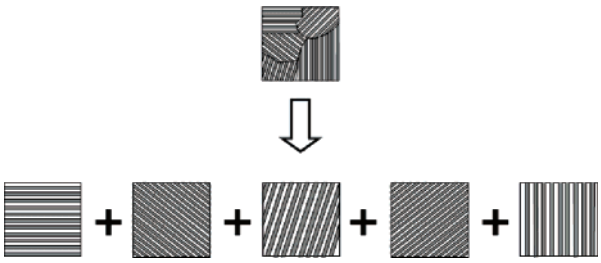

Figure 12. Schematic showing arrangement of lamellar grains in an isotropic sample (top). Cartoons of "single crystal" samples oriented in various directions are shown below.

in the A block of a cylinder-forming ABABA pentablock copolymer and predicted that this fraction can be increased by increasing the length of the middle A block.[14] Qualitatively similar behavior is expected in lamellae-forming systems as well.[38] Increasing the length of the middle block is expected to reduce the entropic chain stretching penalty in the center E block, thus increasing the probability of having bridging conformations in the E domains. Further, a higher bridge-to-loop ratio is expected to improve the connectivity across lamellar domains and result in enhanced toughness at constant ψ_E.[14] To test this hypothesis, we prepared ECECE-10, a block copolymer with a middle-to-end E block ratio ($N_{2,E}/N_{1,E}$) of 2.6. Indeed, this polymer displays a remarkably higher failure strain ($\epsilon_f \approx$ 75%) than ECECE-5 ($\epsilon_f \approx 1\%$) and clearly does not follow the response anticipated by our ϵ_f vs ψ_E plot (Figure 4). Changing the symmetry of the ECECE molecule thus provides an additional pathway to avert brittle failure. In other words, we are able to "shift" the brittle-to-ductile transition to a lower ψ_E than identified for $N_{2,E}/N_{2,E} = 1$. In recent studies, Takano et al. blended cyclic SI diblock copolymer with linear SIS triblock copolymer to manipulate the extent of bridging.[39,40] They reported a decrease in breaking stress with the addition of cyclic SI (expected to reduce the fraction of bridged chains), supporting the idea that the amount of bridging chains can be directly correlated with tensile strength (and toughness).

We have seen a similar dependence on chain architecture (i.e., anchoring of the soft block) in isotropic CPC and PCPCP block copolymers, where P, or poly(ethylene-*alt*-propylene), is a rubbery polymer with no crystallinity.[41]

Deformation of Aligned Samples. The mechanical response of isotropic (polydomain) samples reflects the deformation of numerous lamellae with a uniform distribution of orientations (Figure 12). Motivated by this idea, we shear aligned ECECE-5, CEC-2, and CECEC block copolymers and performed tensile testing along different directions relative to the lamellar orientation.

Lack of toughness in the semicrystalline block makes the ECECE material brittle regardless of lamellar orientation. Experiments on the aligned CEC block copolymer reveal two distinct modes of deformation as a function of orientation. Brittle failure perpendicular to the strain direction for $\theta_{vx} = 0°$ (reported earlier[10,11]) implies a "weak" plane parallel to the plane of the lamellae, and failure likely occurs by C chain pullout, or crack propagation through the C layers, in this orientation. The same mechanism is proposed to operate for $\theta_{vx} = 14°$, based on the direction of failure clearly evident from the pictures of failed tensile bars in Figure 10. For $\theta_{vx} \geq 27°$, samples resist brittle fracture by macroscopic rotation of lamellar grains, as shown by the 2-D SAXS patterns obtained from the $x-z$ plane of failed specimens (Figure 8). This grain rotation must be achieved by shearing of lamellae past one another. There appears to be a critical angle close to 27°, where the deformation mechanism changes from brittle fracture to yielding by shearing of lamellae. It is also clear from Figure 7 that, of all the possible lamellar orientations, a majority ($27° \leq \theta_{vx} \leq 90°$) accommodate strain via grain rotation and avoid brittle fracture. Hence, the isotropic CEC material (some combination of individual orientations) is ductile and actually fails at a strain of nearly 300%. The enhanced toughness of polydomain CEC compared to aligned or "single-crystal" specimens, at any θ_{vx}, indicates that grain boundaries do not detract from the inherent toughness of this material. In fact, the strain at break for the polydomain specimens is greater than the average over all single-crystal values.

The CECEC architecture places bridging (and looping) chains in the C domains, resulting in dramatically higher toughness (compared to CEC) perpendicular to the lamellae normal and nearly "orientation-independent" mechanical properties. The absence of scattering in the q_x-q_z plane and appearance of four spot patterns from the edges of failed samples in the low θ_{vx} limit indicates that the CECEC material accommodates strain by buckling of lamellae, thus preventing brittle fracture. It is important to keep the sample geometry in mind throughout this discussion. The cross section of the tensile bars is 3 mm (x) $\times$ 1 mm (y); hence, the lamellae buckle across the thin dimension. The asymmetry in the sample geometry (rectangular cross section vs square cross section) forces chevron formation across the thin dimension. Cohen et al. reported formation of the chevron morphology in *both* faces when they strained aligned SBS triblock copolymer specimens having square cross sections.[42] For $\theta_{vx} \geq 27°$, shearing motion is activated, and macroscopic grain rotation occurs (evidenced by scattering spots in the q_x-q_z plane), as in the CEC triblock. The weakening of scattering intensities for $\theta_{vx} = 76°$ and 90° in both polymers may be related to fragmentation of PCHE domains and eventual destruction of the lamellar microstructure.[42] The modes of lamellae deformation in aligned CEC and CECEC polymers are summarized in Figure 13. For $\theta_{vx} \leq 14°$, CEC undergoes brittle failure (with no change in microstructure), while CECEC avoids brittle fracture by buckling of lamellae. For $\theta_{vx} \geq 27°$, both polymers accommodate strain by macroscopic rotation of lamellae and display ductile behavior.

It is instructive that the onset of grain rotation occurs between 14° and 27° for both CEC and CECEC block copolymers. From Figure 6, the applied tensile force in a stress−strain experiment can be resolved into normal (N) and shear (τ) components relative to the C/E lamellar interface: $N = \sigma \cos^2 \theta_{vx}$ and $\tau = \sigma \cos \theta_{vx} \sin \theta_{vx}$, where σ is the measured tensile stress.[43] Using a yield stress value of $\sigma_Y \approx 15$ MPa (based on our tensile data), $\tau(\theta_{vx} = 27°) \approx 6$ MPa. If grain rotation is assumed to occur by

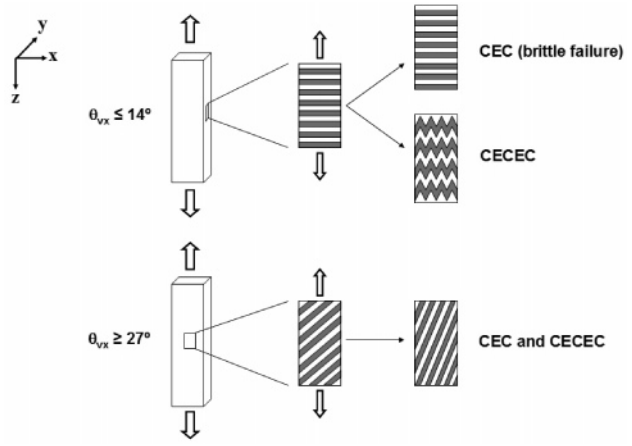

Figure 13. Summary of the modes of deformation in aligned CEC and CECEC block copolymers. For $\theta_{vx} \leq 14°$, CEC undergoes brittle failure (with no change in microstructure), while CECEC avoids brittle fracture by buckling of lamellae. For $\theta_{vx} \geq 27°$, both polymers accommodate ductile strain by macroscopic rotation of lamellae.

sliding of the semicrystalline E domains (and not the rigid C domains), the resistance to sliding likely comes from the polyethylene crystals. Studies using aligned high-density polyethylene (HDPE, $x_C \approx 70\%$) report critical resolved shear stress (CRSS) values for a polyethylene crystal between 6 and 9 MPa,[44−46] close to the τ we estimated above. Since this value only depends on the properties of the polyethylene crystal, it must be independent of chain architecture (CEC or CECEC), and this is indeed what the 2-D SAXS patterns indicate. The relatively weak scattering patterns in the q_x-q_z plane for $\theta_{vx} = 27°$ from both CEC and CECEC specimens suggest a transition in the mode of lamellar deformation close to this angle.

The chevron pattern has been reported in perpendicular deformation of block copolymers composed of alternating glassy and rubbery domains.[10,11,42,47,48] In a study involving deformation of SBS triblock copolymers in a "diagonal" direction (equivalent to $\theta_{vx} = 45°$ by our notation), Cohen et al. also saw macroscopic rotation of lamellae.[42] The absence of a "weak" direction in the material they employed ($M_S \approx M_{e,S}$, in their S blocks) led to nearly identical toughness for all orientations.

In summary, Figures 4 and 7 describe the toughness of isotropic and aligned C/E block copolymers spanning a wide range of architectures. Brittle failure (independent of lamellae orientation) results when an insufficient number of E chains are anchored at C/E interfaces. Toughening is achieved by progressively pinning down E chains (mathematically described by ψ_E), and for all architectures with $\psi_E > 0.8$, a failure strain of ~300% is seen in isotropic samples. The CEC architecture represents the simplest example of tying down all E chains ($\psi_E = 1$). However, Figure 7 reveals the existence of a weak direction in the CEC material and is attributed to loose C chains. The CECEC architecture places enough bridging C chains to alleviate this deficiency, and a nearly "orientation independent" tough material (with $\epsilon_f \sim 300\%$) is obtained. Employing various molecular architectures has enabled us to understand the role of chain conformations in both semicrystalline and glassy domains. Tensile properties of isotropic materials depend critically on the degree of anchoring in the soft block (Figure 4). In addition, bridging conformations in the hard block have a dramatic effect on macroscopically aligned materials (Figure 7). Thus, the CE diblock and CECEC pentablock architectures represent the brittle and tough limits (regardless of lamellae orientation) in C/E block copolymers. With this study, we have been able to dichotomize the mechanical effects of manipulating chain conformations in the C and E blocks by systematic variation of block copolymer architecture.

Additionally, we have demonstrated the crucial role of block size symmetry in multiblock copolymers. Tensile properties of the ECECE-10 material ($N_{2,E} \approx 2.6N_{1,E}$) clearly show a departure from the "universal" description provided in Figure 4. Thus, the reinforcement of E domains for $0.6 < \psi_E < 0.8$ in the blend specimens fails to account for the properties of a block copolymer with a different symmetry ($N_{2,E}/N_{1,E}$). This strongly implies a higher bridging fraction in the center E block in ECECE-10 compared to the other samples employed. We are currently exploring the effect of block symmetry in greater detail by studying materials with varying $N_{2,E}/N_{1,E}$. As this ratio is increased, we expect that a critical value of $N_{2,E}/N_{1,E}$ will be reached, when the E end blocks may mix with the C domains, resulting in a C′EC′ triblock copolymer (where C′ represents PCHE diluted with short E blocks).

Conclusions

This paper describes the mechanical properties of a number of glassy−semicrystalline block copolymers. Tri-, tetra-, and pentablock copolymers with varying block sequences were employed to manipulate chain conformations in the semicrystalline and glassy domains. A single molecular parameter related to the degree of chain bridging was identified that appears to be universally correlated with failure strain (toughness), independent of block copolymer architecture for a given block size symmetry. Studies on macroscopically aligned specimens provided further insight into the role of chain architecture and mechanisms of lamellae deformation. We believe the principles of fracture toughness revealed by this work should apply to other "hard−soft" block copolymer systems.

Acknowledgment. This work was supported by Cummins Inc. and the National Science Foundation's Research Experience for Undergraduates (NSF-REU) program. Characterization facilities used in this work were partially supported by the NSF sponsored Materials Research Science and Engineering Center (MRSEC) at the University of Minnesota. We thank Steve Hahn at the Dow Chemical Co. for generously providing the CEC and CECEC block copolymers used in this study. We sincerely appreciate stimulating conversations with Marc Hillmyer, Glenn Fredrickson, and Mark Matsen. Qiang Lan is acknowledged for help with using the DMA-7e rheometer. We are grateful for the helpful insight provided by discussions with Mahesh Mahanthappa.

References and Notes

(1) Holden, G.; Legge, N. R.; Quirk, R. P.; Schroeder, H. E. In *Thermoplastic Elastomers*, 2nd ed.; Hanser/Gardner Publications: Cincinnati, OH, 1996; p 69.
(2) Lodge, T. P. *Macromol. Chem. Phys.* **2003**, *204*, 265−273.
(3) Spontak, R. J.; Patel, N. P. *Curr. Opin. Colloid Interface Sci.* **2000**, *5*, 334−341.
(4) Hartsock, D. L.; Stacy, N. E. In *Modern Styrenic Polymers: Polystyrenes and Styrenic Copolymers*, 1st ed.; John Wiley and Sons Ltd.: Chichester, UK, 2003; p 501.
(5) Zhao, J.; Hahn, S. F.; Hucul, D. A.; Meunier, D. M. *Macromolecules* **2001**, *34*, 1737−1741.
(6) Hucul, D. A.; Hahn, S. F. *Adv. Mater.* **2000**, *12*, 1855−1858.
(7) Fetters, L. J.; Lohse, D. J.; Richter, D.; Witten, T. A.; Zirkel, A. *Macromolecules* **1994**, *27*, 4639−4647.
(8) Bates, F. S.; Fredrickson, G. H.; Hucul, D.; Hahn, S. F. *AIChE J.* **2001**, *47*, 762−765.
(9) Cochran, E. W.; Bates, F. S. *Macromolecules* **2002**, *35*, 7368−7374.
(10) Mori, Y.; Lim, L. S.; Bates, F. S. *Macromolecules* **2003**, *36*, 9879−9888.
(11) Hermel, T. J.; Hahn, S. F.; Chaffin, K. A.; Gerberich, W. W.; Bates, F. S. *Macromolecules* **2003**, *36*, 2190−2193.

(12) Khanna, V.; Ruokolainen, J.; Kramer, E. J.; Hahn, S. F. *Macromolecules* **2006**, *39*, 4480−4492.
(13) Ryu, C. Y.; Ruokolainen, J.; Fredrickson, G. H.; Kramer, E. J.; Hahn, S. F. *Macromolecules* **2002**, *35*, 2157−2166.
(14) Drolet, F.; Fredrickson, G. H. *Macromolecules* **2001**, *34*, 5317−5324.
(15) Ruokolainen, J.; Fredrickson, G. H.; Kramer, E. J.; Ryu, C. Y.; Hahn, S. F.; Magonov, S. N. *Macromolecules* **2002**, *35*, 9391−9402.
(16) It should be noted that in the *isotropic* lamellar arrangement both CEC and CECEC block copolymers display ductile behavior and fail at nearly identical strains.[28]
(17) Lim, L. S.; Harada, T.; Hillmyer, M. A.; Bates, F. S. *Macromolecules* **2004**, *37*, 5847−5850.
(18) Kawai, H.; Hashimoto, T.; Miyoshi, K.; Uno, H.; Fujimura, M. *J. Macromol. Sci.* **1980**, *B17*, 427−472.
(19) Matsuo, M.; Ueno, T.; Horino, H.; Chujyo, S.; Asai, H. *Polymer* **1968**, *9*, 425−436.
(20) Koppi, K. A.; Tirrell, M.; Bates, F. S.; Almdal, K.; Colby, R. H. *J. Phys. II* **1992**, *2*, 1941−1959.
(21) Ndoni, S.; Papadakis, C. M.; Bates, F. S.; Almdal, K. *Rev. Sci. Instrum.* **1995**, *68*, 1090−1095.
(22) Koppi, K. A. Ph.D. Thesis, University of Minnesota, Minneapolis, 1993.
(23) Hermel, T. J.; Wu, L.; Hahn, S. F.; Lodge, T. P.; Bates, F. S. *Macromolecules* **2002**, *35*, 4685-4689.
(24) Bailey, T. S. Ph.D. Thesis, University of Minnesota, Minneapolis, 2001.
(25) Hillmyer, M. A.; Bates, F. S. *Macromolecules* **1996**, *29*, 6994−7002.
(26) Rosedale, J. H.; Bates, F. S. *Macromolecules* **1990**, *23*, 2329−2338.
(27) Khandpur, A. K.; Forster, S.; Bates, F. S.; Hamley, I. W.; Ryan, A. J.; Bras, W.; Almdal, K.; Mortensen, K. *Macromolecules* **1995**, *28*, 8796−8806.
(28) Brandrup, J., Immergut, E. H., Eds.; *Polymer Handbook*, 3rd ed.; Wiley: New York, 1989.
(29) Weimann, P. A.; Hajduk, D. A.; Chu, C.; Chaffin, K. A.; Brodil, J. C.; Bates, F. S. *J. Polym. Sci., Part B* **1999**, *37*, 2053−2068.
(30) Hermel, T. J. Ph.D. Thesis, University of Minnesota, Minneapolis, 2003.
(31) Phatak, A.; Macosko, C. W.; Bates, F. S.; Hahn, S. F. *J. Rheol.* **2005**, *49*, 197−214.
(32) Matsen, M. W. *J. Chem. Phys.* **1995**, *102*, 3884−3887.
(33) Matsen, M. W.; Schick, M. *Macromolecules* **1994**, *27*, 187−192.
(34) Jones, R. L.; Kane, L.; Spontak, R. J. *Chem. Eng. Sci.* **1996**, *51*, 1365−1375.
(35) Karatasos, K.; Anastasiadis, S. H.; Pakula, T.; Watanabe, H. *Macromolecules* **2000**, *33*, 523−541.
(36) Watanabe, H. *Macromolecules* **1995**, *28*, 5006−5011.
(37) Watanabe, H.; Tan, H. *Macromolecules* **2004**, *37*, 5118−5122.
(38) Matsen, M. W. Personal communication.
(39) Takano, A.; Kamaya, I.; Takahashi, Y.; Matsushita, Y. *Macromolecules* **2005**, *38*, 9718−9723.
(40) Takahashi, Y.; Song, Y.; Nemoto, N.; Takano, A.; Akazawa, Y.; Matsushita, Y. *Macromolecules* **2005**, *38*, 9724−9729.
(41) Lim, L. S. Ph.D. Thesis, University of Minnesota, Minneapolis, MN, 2005.
(42) Cohen, Y.; Albalak, R. J.; Dair, B. J.; Capel, M.; Thomas, E. L. *Macromolecules* **2000**, *33*, 6502−6516.
(43) Callister, W. D. In *Materials Science and Engineering—An Introduction*, 5th ed.; John Wiley and Sons: New York, 2000; p 160.
(44) Bartczak, Z.; Argon, A. S.; Cohen, R. E. *Macromolecules* **1992**, *25*, 5036−5053.
(45) Bartczak, Z.; Cohen, R. E.; Argon, A. S. *Macromolecules* **1992**, *25*, 4692−4704.
(46) Young, R. J.; Bowden, P. B.; Ritchie, J. M.; Rider, J. G. *J. Mater. Sci.* **1973**, *8*, 23−36.
(47) Cohen, Y.; Brinkmann, M.; Thomas, E. L. *J. Chem. Phys.* **2001**, *114*, 984−992.
(48) Cohen, Y.; Thomas, E. L. *Macromolecules* **2003**, *36*, 5265−5270.

MA0611319